

Circ-RPL15/miR-146b-3p/VEGFA feedback loop is responsible for triggering proliferation and migration in glioma

B. WANG¹, R. DUAN¹, Z.-B. LI², L. WANG²

¹Department of Neurosurgery, Peking University International Hospital, Beijing, China

²Department of Neurosurgery, Beijing Tiantan Hospital, Capital Medical University, Beijing, China

Bin Wang and Ran Duan contributed equally to this work

Abstract. – OBJECTIVE: This study aims to elucidate the role of circ-RPL15 in the progression of glioma.

PATIENTS AND METHODS: Circ-RPL15 levels in glioma tissues and normal brain tissues were detected. Subcellular distribution of circ-RPL15 was examined. The binding between miR-146b-3p and circ-RPL15 was verified by Luciferase assay. Potential targets of miR-146b-3p were further determined. The influences of the circ-RPL15/miR-146b-3p/VEGFA feedback loop on proliferative and migratory abilities in T98G and U251 cells were detected by cell counting kit-8 (CCK-8) and transwell assay, respectively.

RESULTS: Circ-RPL15 and VEGFA were upregulated in glioma tissues than normal ones, whereas miR-146b-3p was downregulated. Circ-RPL15 was mainly distributed in the cytoplasm. The interaction in the circ-RPL15/miR-146b-3p/VEGFA feedback loop was indicated by Luciferase assay, and it markedly promoted proliferative and migratory abilities in glioma.

CONCLUSIONS: Circ-RPL15 triggers proliferative and migratory potentials in glioma by competitively binding miR-146b-3p and thus upregulates VEGFA.

Key Words:

Glioma, Circ-RPL15/miR-146b-3p/VEGFA feedback loop, Proliferation, Migration.

Introduction

Glioma is a common primary brain tumor that starts from glial cells of the brain or the spinal cord. The annual incidence of glioma is about 3-8/100,000. It is classified into grade I-IV. As a fatal disease, glioma is featured by high morbidity, high recurrence rate, and high mor-

talidity, especially anaplastic astrocytoma (WHO grade III) and glioblastoma (WHO grade IV)¹. Anaplastic astrocytoma is a diffuse infiltrating tumor. Compared with low-grade astrocytoma, it is featured by dispersive anaplasia and increased proliferation index².

The pathogenesis of glioma involves both internal and external factors, including genetic susceptibilities and environmental factors. At the cellular level, mutations in genetic factors create a favorable microenvironment where cells are evaded from normal apoptosis and cell metabolism. Uncontrolled cell proliferation thereafter causes tumor cell growth, neovascularization, hypoxia, and necrosis³. Currently, surgical resection to the extent feasible and postoperative radiotherapy are preferred to glioma patients. For high-grade glioma, surgical resection cannot completely remove tumor lesions, and both chemotherapy and radiotherapy are necessary after the surgery. Growing evidence has shown promising applications of immunotherapy, targeted therapy, and gene therapy for glioma in recent years.

CircRNAs are functional in regulating RNA expressions, protein translation, protein activities and post-transcriptional mediation. Yang et al⁴ showed that circRNAs with IRES insertion can translate peptides in cells, so can those with abundant m⁶A modifications. It is reported that circZNF292 promotes tubular formation of glioma cells by activating the Wnt pathway⁵. Glioma cell adhesion and growth are stimulated by hsa_circ_0000177 in the Wnt-dependent way. CircNT5E is overexpressed in glioma cells, which drives the growth and metastasis of U251 cells by acting as a ceRNA for miR-422a⁶. A

previous study has shown that circ-RPL15 is highly expressed in plasma exosomes of chronic lymphocyte leukemia cases. Its potential function in glioma progression remains unclear.

VEGFA is reported to be upregulated in glioma profiling. CircSCAF11 triggers glioma by the miR-421/SP1/VEGFA axis⁷. We explored the interaction in circ-RPL15/miR-146b-3p/VEGFA feedback loop and its involvement in glioma.

Patients and Methods

Patients

Paraffin-embedded glioma tissues (n=38) and normal brain tissues (n=38) were collected from glioma patients treated in Peking University International Hospital from January 2011 to October 2019. A total of 17 male patients and 21 females with 29-78 years were recruited, involving 9 well differentiated, 12 moderately differentiated and 17 poorly differentiated cases. There were 19/38 glioma patients accompanied lymphatic metastases. Tumor pathological classification and staging standards are implemented in accordance with the staging standards of the Union for International Cancer Control (UICC). All participants were not treated with radiotherapy and chemotherapy before operation. Tumor tissues diagnosed with glioma were confirmed by the pathologist in our hospital. Other kind of tumor that migrated to the brain was excluded. This investigation was approved by the Ethics Committee of Peking University International Hospital and it was conducted after informed consent of each subject.

Cell Culture and Transfection

Glioma cell lines were cultured in Dulbecco's Modified Eagle's Medium (DMEM; Gibco,

Rockville, MD, USA) with 10% fetal bovine serum (FBS; Gibco, Rockville, MD, USA). Cells were cultured to 50-70% density and transfected using Lipofectamine 2000 (Invitrogen, Carlsbad, CA, USA). Fresh medium was replaced at 4-6 h. Transfected cells for 48 h were used for following experiments.

Quantitative Real Time-Polymerase Chain Reaction (qRT-PCR)

Total RNA was extracted from cell lysate using TRIzol reagent (Invitrogen, Carlsbad, CA, USA) and purified. It was reversely transcribed into complementary deoxyribose nucleic acid (cDNA) using the PrimeScript RT reagent Kit (TaKaRa, Dalian, China). The cDNA was subjected to qRT-PCR using the SYBR Green Master Mix (Applied Biosystems, San Diego, CA, USA). Primer sequences were listed in Table I.

Cell Proliferation Assay

Cells were inoculated in a 96-well plate with 2×10^3 cells per well. At the appointed time points, absorbance value at 490 nm of each sample was recorded using the cell counting kit-8 (CCK-8) kit (RIBOBIO, Guangzhou, China) for plotting the viability curves.

Transwell Assay

Transwell chambers (Millipore, Billerica, MA, USA) were inserted in each well of a 24-well plate. 200 μ L of suspension (3×10^4 cells/mL) was applied in the upper layer of the chamber with 600 μ L of medium containing 20% FBS in the bottom. After 48-h incubation, migratory cells in the bottom were reacted with 15-min methanol, 20-min crystal violet and captured using a microscope (Olympus, Tokyo, Japan). Migratory cells were counted in 10 random selected fields per sample.

Table I. Primer sequences of plasmids used in qRT-PCR.

Gene	Primer sequences
circ-RPL15	F: 5'-CCTTCAGTAAGCCAAGAT-3' R: 5'-GCTCGAAGCCTTCAGTAAG-3'
VEGFA	F: 5'-AGGGCAGAATCATCACGAAGT-3' R: 5'-AGGGTCTCGATTGGATGGCA-3'
miR-146b-3p	F: 5'-ACACTCCAGCTGGGGGTCTTGACTCAGGTG-3' R: 5'-CTCAACTGGTGTCTGTGGAGTCGGCAATTCAGTTGAGACGGGACA-3'
GAPDH	F: 5'-TCCTCCACCTTTGATGCG-3' R: 5'-GTGCCTGGCTCACTCCTT-3'
U6	F: 5'-CTCGCTTCGGCAGCACA-3' R: 5'-AACGCTTCACGAATTTGCGT-3'

Luciferase Assay

The cells were co-transfected with wild-type pGL3-circ-RPL15/mutant-type pGL3-circ-RPL15 and negative control/miR-146b-3p mimics. Cells were lysed in Dual-Glo[®] Luciferase Reagent (Promega, Madison, WI, USA) for 10 min, followed by luciferase activity measurement.

Subcellular Distribution Analysis

The cells were lysed in 100 μ L of Buffer A (10 mM HEPES, pH 7.9, 10 mM KCl, 0.1 mM EDTA (ethylenediaminetetraacetic acid), 0.1 mM EGTA, 0.15% NP-40) on ice for 15 min. Subsequently, the mixture was centrifuged at 4°C, 12000 rpm for 1 min. The supernatant was collected as the cytoplasmic fraction. The precipitant was washed in 1 mL of Buffer A for three times, and re-suspended in 150 μ L of Buffer B (20 mM HEPES, pH 7.9, 0.4 mM NaCl, 1 mM EDTA, 1 mM EGTA, 0.5% NP-40). After 30-min centrifugation at 4°C, 12000 rpm, the supernatant was collected as the nuclear fraction. The mRNA level of circ-RPL15 in each fraction was detected by qRT-PCR.

Statistical Analysis

Stata 9.2 software (London, UK) was used for data analysis. Data were expressed as mean \pm standard deviation. Differences between groups were analyzed by the two-tailed *t*-test. Pearson correlation test was applied for assessing correlation between two genes. *p*<0.05 was considered as statistically significant.

Results

Circ-RPL15 Was Upregulated In Glioma Profiling

Compared with normal brain tissues (n=38), circ-RPL15 was upregulated in glioma tissues (n=38) (Figure 1A). Based on the tumor size, glioma tissues were classified into large group (≥ 3 cm, n=21) and small group (<3 cm, n=17). Higher level of circ-RPL15 was detected in the large group (Figure 1B). Similarly, circ-RPL15 was highly expressed in glioma cell lines (Figure 1C).

Circ-RPL15 Promoted Proliferative and Migratory Abilities in Glioma

CCK-8 results showed that knockdown of circ-RPL15 decreased viability in T98G and U251 cells, whereas overexpression of circ-RPL15 achieved the opposite results (Figure 2A, 2C). In addition, knockdown of circ-RPL15 reduced the number of migratory glioma cells, which was enhanced by overexpression of circ-RPL15 (Figure 2B, 2D).

The Negative Interaction Between MiR-146b-3p and Circ-RPL15

Converse to the expression pattern of circ-RPL15, miR-146b-3p was downregulated in glioma tissues (Figure 3A), especially those with larger tumor size (Figure 3B). We identified a negative correlation between levels of circ-RPL15 and miR-146b-3p in glioma tissues ($R^2=0.1472$, *p*=0.0174, Figure 3C). Through analyzing sub-cellular distribution, circ-RPL15 was found to be mainly distributed in the cytoplasm of T98G

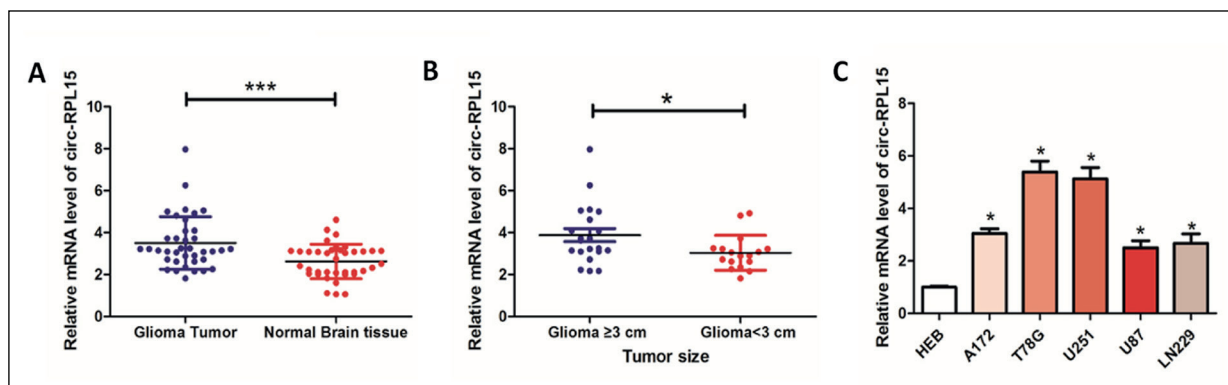


Figure 1. Circ-RPL15 was upregulated in glioma profiling. **A**, Circ-RPL15 levels in glioma tissues (n=38) and normal brain tissues (n=38). **B**, Circ-RPL15 levels in glioma tissues with ≥ 3 cm in tumor size (n=21) and those with <3 cm (n=17). **C**, Circ-RPL15 levels in glioma cell lines.

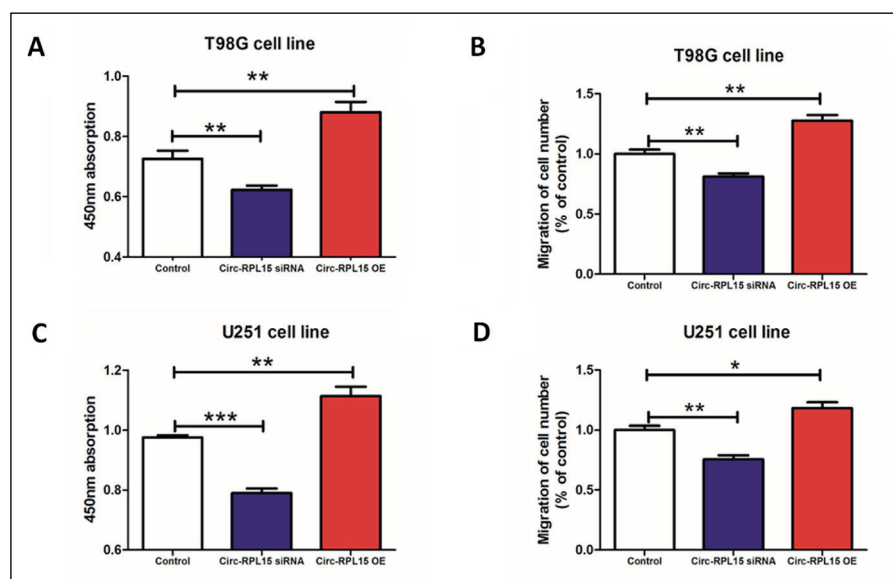


Figure 2. Circ-RPL15 promoted proliferative and migratory abilities in glioma. **A**, Viability in T98G cells regulated by circ-RPL15. **B**, Migration in T98G cells regulated by circ-RPL15. **C**, Viability in U251 cells regulated by circ-RPL15. **D**, Migration in U251 cells regulated by circ-RPL15.

and U251 cells, predicting the potential function of circ-RPL15 in miRNA sponge (Figure 3D). Subsequently, wild-type and mutant-type pGL3-circ-RPL15 vectors were constructed according to the predicted binding sequence in the

3'UTR of circ-RPL15 and miR-146b-3p (Figure 3E). Transfection of miR-146b-3p mimics largely decreased Luciferase activity in the wild-type pGL3-circ-RPL15, verifying the binding between circ-RPL15 and miR-146b-3p (Figure 3F).

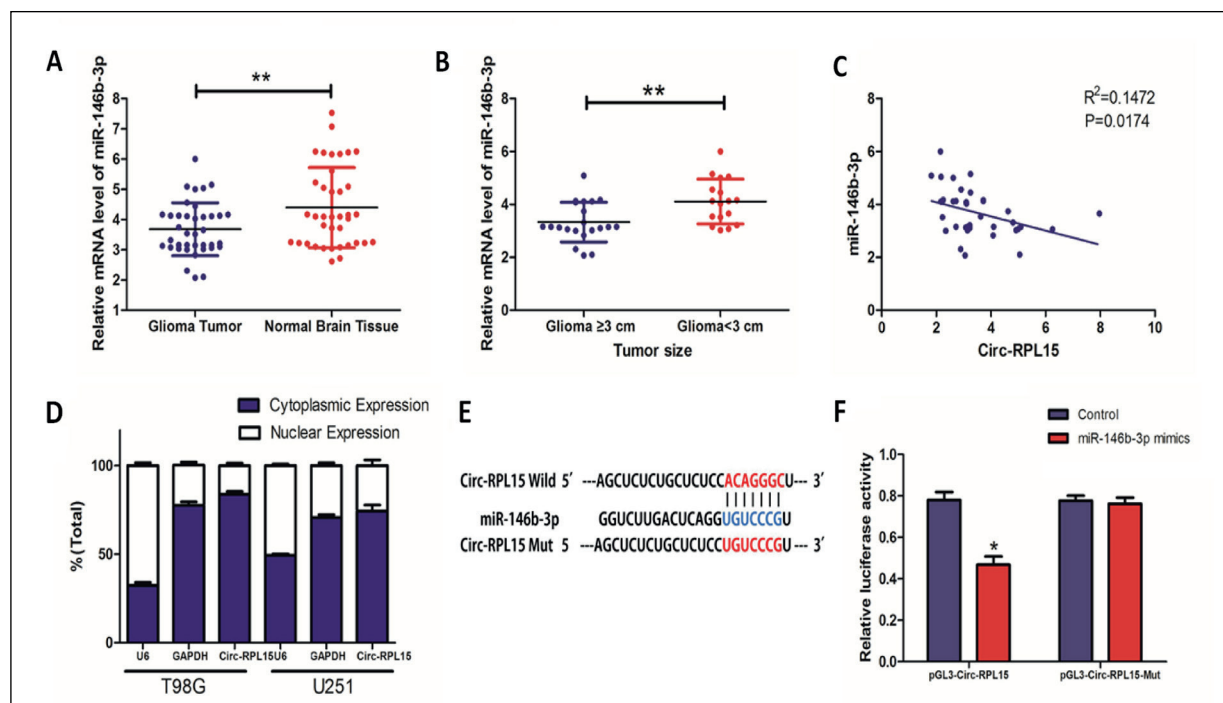


Figure 3. The negative interaction between miR-146b-3p and circ-RPL15. **A**, MiR-146b-3p levels in glioma tissues (n=38) and normal brain tissues (n=38). **B**, MiR-146b-3p levels in glioma tissues with ≥ 3 cm in tumor size (n=21) and those with < 3 cm (n=17). **C**, A negative correlation between levels of circ-RPL15 and miR-146b-3p in glioma tissues ($R^2=0.1472$, $p=0.0174$). **D**, Subcellular distribution of circ-RPL15 in T98G and U251 cells. **E**, The predicted binding sequence in the 3'UTR of circ-RPL15 and miR-146b-3p. **F**, Luciferase activity in cells co-transfected with miR-146b-3p mimics/negative control and wild-type/mutant-type pGL3-circ-RPL15 vectors.

Circ-RPL15/MiR-146b-3p/VEGFA Feedback Loop Was Responsible for Regulating Glioma Progression

VEGFA was found to be upregulated in glioma tissues (Figure 4A), and displayed a negative correlation to miR-146b-3p level ($R^2=0.2307$, $p=0.0023$, Figure 4B). However, VEGFA level was positively correlated to circ-RPL15 level ($R^2=0.2735$, $p=0.008$, Figure 4C).

We thereafter explored the involvement of miR-146b-3p in circ-RPL15-regulated glioma cell phenotypes. First of all, VEGFA was downregulated in T98G and U251 cells overexpressing miR-146b-3p. Its level remained higher in glioma cells co-overexpressing circ-RPL15 and miR-146b-3p than those with miR-146b-3p overexpression (Figure 5A, 5D). Overexpression of miR-146b-3p reduced viability in glioma cells, and the inhibited viability was relieved by overexpressed circ-RPL15 (Figure 5B, 5E). As expected, overexpression of circ-RPL15 was able to abolish the regulatory effect of miR-146b-3p on migratory potential in glioma cells (Figure 5C, 5F).

Discussion

Glioma is a highly malignant tumor with only 14.6 months of median survival after diagnosis⁸. Although glioma patients can be treated by surgery and postoperative adjuvant therapy, their overall survival ranges 12-18 months⁹⁻¹¹. Strong invasive and migratory abilities of glioma cells attribute to the poor prognosis in glioma patients¹². At present, molecular mechanisms and biomarkers of glioma have been extensively studied. Target therapy has been emerged for alleviating the progression of glioma¹³.

CircRNAs are critical regulators involved in tumor progression. They are capable of regulating almost every aspect of tumor cell behavior¹⁴. CircRNAs are subtyped into ecircRNAs, ciRNAs and EiciRNAs. As a special non-coding RNA, circRNA does not have 5' and 3' end. It is structurally formed by a covalently closed loop. Because the special structure, circRNAs are highly stable and resistant to exonuclease degradation. Biological functions of circRNAs are achieved by the effect of miRNA sponges or interaction with RNA-binding proteins¹⁵. Wu et al¹⁶ has demonstrated the role of circ-RPL15 in the chronic lymphocytic leukemia. Our findings uncovered that circ-RPL15 was upregulated in glioma tissues, especially those with larger tumor size. Overexpression of circ-RPL15 remarkably stimulated proliferative and migratory abilities in both T98G and U251 cells. Since circ-RPL15 was detected to be mainly distributed in the cytoplasm, we believed that its biological function relied on the post-transcriptional regulation on target genes. Bioinformatics analysis depicted the binding sequence in the 3'UTR of circ-RPL15 and miR-146b-3p, and their binding relationship was further proved by Luciferase assay. Of note, miR-146b-3p was able to abolish the regulatory effects of circ-RPL15 on glioma cell phenotypes. Therefore, circ-RPL15 might function as a ceRNA to exert a sponge effect on miR-146b-3p, thus promoting the malignant progression of glioma.

Angiogenesis is a process in which new blood vessels are formed from existing capillaries or veins behind capillaries. It is a necessary and complex process for the growth and metastasis of many malignant tumors. VEGFA, as the most important angiogenic factor, is a vital protein

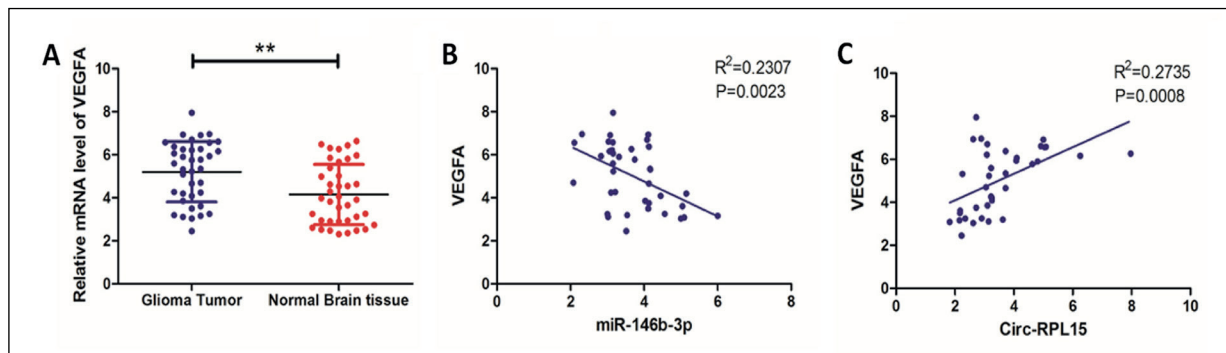


Figure 4. The interaction among circ-RPL15, miR-146b-3p and VEGFA. **A**, VEGFA levels in glioma tissues (n=38) and normal brain tissues (n=38). **B**, A negative correlation between levels of VEGFA and miR-146b-3p in glioma tissues ($R^2=0.2307$, $p=0.0023$). **C**, A positive correlation between levels of VEGFA and circ-RPL15 in glioma tissues ($R^2=0.2735$, $p=0.0008$).

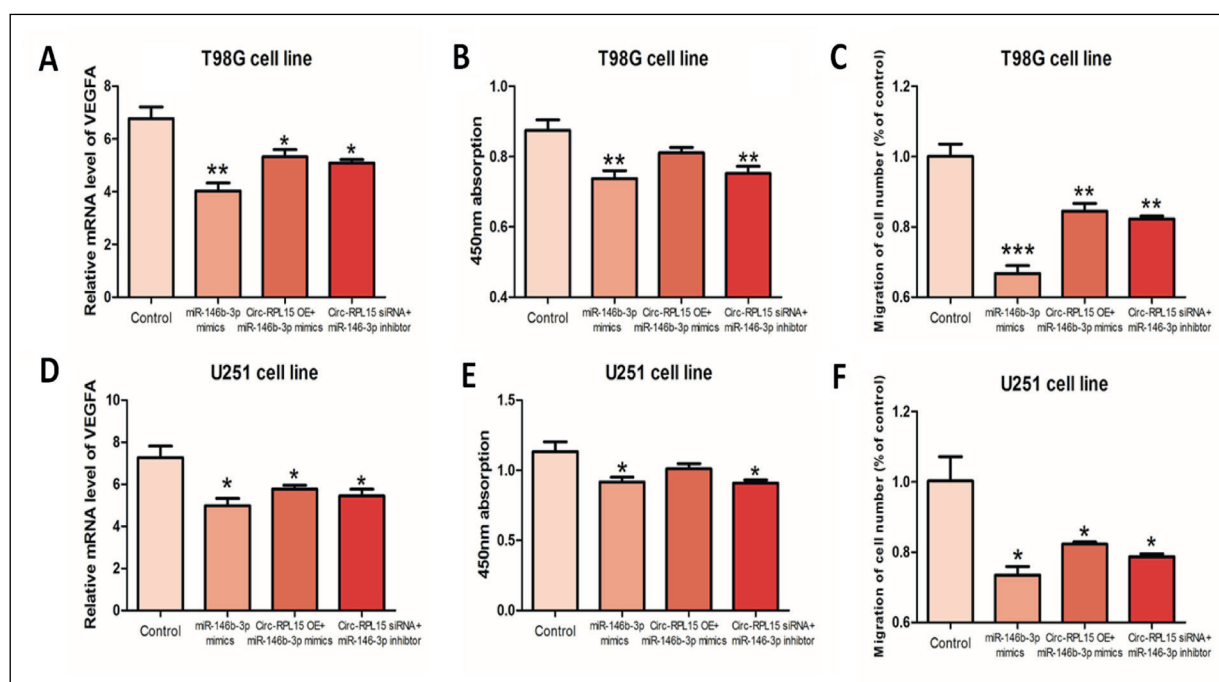


Figure 5. Circ-RPL15/miR-146b-3p/VEGFA feedback loop was responsible for regulating glioma progression. **A**, VEGFA level in T98G cells transfected with miR-146b-3p mimics, circ-RPL15 OE + miR-146b-3p mimics, or circ-RPL15 siRNA + miR-146b-3p inhibitor. **B**, Viability in T98G cells transfected with miR-146b-3p mimics, circ-RPL15 OE + miR-146b-3p mimics, or circ-RPL15 siRNA + miR-146b-3p inhibitor. **C**, Migration in T98G cells transfected with miR-146b-3p mimics, circ-RPL15 OE + miR-146b-3p mimics, or circ-RPL15 siRNA + miR-146b-3p inhibitor. **D**, VEGFA level in U251 cells transfected with miR-146b-3p mimics, circ-RPL15 OE + miR-146b-3p mimics, or circ-RPL15 siRNA + miR-146b-3p inhibitor. **E**, Viability in U251 cells transfected with miR-146b-3p mimics, circ-RPL15 OE + miR-146b-3p mimics, or circ-RPL15 siRNA + miR-146b-3p inhibitor. **F**, Migration in U251 cells transfected with miR-146b-3p mimics, circ-RPL15 OE + miR-146b-3p mimics, or circ-RPL15 siRNA + miR-146b-3p inhibitor.

responsible for initiating angiogenesis, and has become a therapeutic target for diseases with abnormal angiogenesis. It stimulates epithelium proliferation and enhances vascular permeability. It is reported that VEGFA is upregulated in lung cancer tissues. MiR-195 suppresses lung cancer cell metastasis by downregulating VEGFA¹⁷. Cao et al¹⁸ demonstrated that VEGFA is upregulated in 86% of bladder cancer patients they recruited. VEGFA level is closely linked to tumor staging, blood vessel invasion, and disease-free survival in bladder cancer patients. The members of VEGF family, including VEGFA, VEGFB, VEGFC, VEGFD and placental growth factor, are important regulators in tumor angiogenesis and metastasis¹⁹. VEGFA has been clearly shown to contribute to the angiogenesis of glioma. New blood vessels in glioma tissues can supply sufficient blood to ensure tumor growth. Hence, VEGFA is essential for the progression of glioma. In glioma tissues we collected, VEGFA was highly expressed than normal

brain tissues. It displayed a positive correlation to circ-RPL15, but a negative correlation to miR-146b-3p level in glioma tissues. This study is expected to provide a new perspective for the occurrence and development mechanism of glioma, and provide new ideas for the clinical diagnosis and treatment of glioma.

Conclusions

Collectively, we have identified the circ-RPL15/miR-146b-3p/VEGFA feedback loop that is responsible for aggravating the progression of glioma.

Conflict of Interest

The Authors declare that they have no conflict of interests.

References

- 1) LOUIS DN, PERRY A, REIFENBERGER G, VON DEIMLING A, FIGARELLA-BRANGER D, CAVENEE WK, OHGAKI H, WIESLER OD, KLEIHUES P, ELLISON DW. The 2016 World Health Organization Classification of Tumors of the Central Nervous System: a summary. *Acta Neuropathol* 2016; 131: 803-820.
- 2) VAN DEN BENT MJ, BAUMERT B, ERRIDGE SC, VOGELBAUM MA, NOWAK AK, SANSON M, BRANDES AA, CLEMENT PM, BAURAIN JF, MASON WP, WHEELER H, CHINOT OL, GILL S, GRIFFIN M, BRACHMAN DG, TAAL W, RUDA R, WELLER M, MCBAIN C, REUNEVELD J, ENTING RH, WEBER DC, LESIMPLE T, CLENTON S, GIJTENBEEK A, PASCOE S, HERRLINGER U, HAU P, DHERMAIN F, VAN HEUVEL I, STUPP R, ALDAPE K, JENKINS RB, DUBBINK HJ, DINJENS W, WESSELING P, NUYENS S, GOLFINOPOULOS V, GORLIA T, WICK W, KROS JM. Interim results from the CATNON trial (EORTC study 26053-22054) of treatment with concurrent and adjuvant temozolomide for 1p/19q non-co-deleted anaplastic glioma: a phase 3, randomised, open-label intergroup study. *Lancet* 2017; 390: 1645-1653.
- 3) CHEN R, SMITH-COHN M, COHEN AL, COLMAN H. Glioma subclassifications and their clinical significance. *Neurotherapeutics* 2017; 14: 284-297.
- 4) YANG Y, FAN X, MAO M, SONG X, WU P, ZHANG Y, JIN Y, YANG Y, CHEN LL, WANG Y, WONG CC, XIAO X, WANG Z. Extensive translation of circular RNAs driven by N(6)-methyladenosine. *Cell Res* 2017; 27: 626-641.
- 5) YANG P, QIU Z, JIANG Y, DONG L, YANG W, GU C, LI G, ZHU Y. Silencing of cZNF292 circular RNA suppresses human glioma tube formation via the Wnt/beta-catenin signaling pathway. *Oncotarget* 2016; 7: 63449-63455.
- 6) WANG R, ZHANG S, CHEN X, LI N, LI J, JIA R, PAN Y, LIANG H. CircNT5E acts as a sponge of mir-422a to promote glioblastoma tumorigenesis. *Cancer Res* 2018; 78: 4812-4825.
- 7) MENG Q, LI S, LIU Y, ZHANG S, JIN J, ZHANG Y, GUO C, LIU B, SUN Y. Circular RNA circSCAF11 accelerates the glioma tumorigenesis through the miR-421/SP1/VEGFA axis. *Mol Ther Nucleic Acids* 2019; 17: 669-677.
- 8) VAN MEIR EG, HADJIPANAYIS CG, NORDEN AD, SHU HK, WEN PY, OLSON JJ. Exciting new advances in neuro-oncology: the avenue to a cure for malignant glioma. *CA Cancer J Clin* 2010; 60: 166-193.
- 9) BERGES R, BALZEAU J, PETERSON AC, EYER J. A tubulin binding peptide targets glioma cells disrupting their microtubules, blocking migration, and inducing apoptosis. *Mol Ther* 2012; 20: 1367-1377.
- 10) LI B, HUANG MZ, WANG XQ, TAO BB, ZHONG J, WANG XH, ZHANG WC, LI ST. TMEM140 is associated with the prognosis of glioma by promoting cell viability and invasion. *J Hematol Oncol* 2015; 8: 89.
- 11) WANG Z, GUO Q, WANG R, XU G, LI P, SUN Y, SHE X, LIU Q, CHEN Q, YU Z, LIU C, XIONG J, LI G, WU M. The D Domain of LRRC4 anchors ERK1/2 in the cytoplasm and competitively inhibits MEK/ERK activation in glioma cells. *J Hematol Oncol* 2016; 9: 130.
- 12) DENG L, LI G, LI R, LIU Q, HE O, ZHANG J. Rho-kinase inhibitor, fasudil, suppresses glioblastoma cell line progression in vitro and in vivo. *Cancer Biol Ther* 2010; 9: 875-884.
- 13) MILLER JJ, WEN PY. Emerging targeted therapies for glioma. *Expert Opin Emerg Drugs* 2016; 21: 441-452.
- 14) ZHU J, YE J, ZHANG L, XIA L, HU H, JIANG H, WAN Z, SHENG F, MA Y, LI W, QIAN J, LUO C. Differential expression of circular RNAs in glioblastoma multiforme and its correlation with prognosis. *Transl Oncol* 2017; 10: 271-279.
- 15) MEMCZAK S, JENS M, ELEFSINIOTI A, TORTI F, KRUEGER J, RYBAK A, MAIER L, MACKOWIAK SD, GREGENSEN LH, MUNSCHAUER M, LOEWER A, ZIEBOLD U, LANDTHALER M, KOCKS C, LE NOBLE F, RAJEWSKY N. Circular RNAs are a large class of animal RNAs with regulatory potency. *Nature* 2013; 495: 333-338.
- 16) WU Z, SUN H, LIU W, ZHU H, FU J, YANG C, FAN L, WANG L, LIU Y, XU W, LI J, JIN H. Circ-RPL15: a plasma circular RNA as novel oncogenic driver to promote progression of chronic lymphocytic leukemia. *Leukemia* 2020; 34: 919-923.
- 17) LIU H, CHEN Y, LI Y, LI C, QIN T, BAI M, ZHANG Z, JIA R, SU Y, WANG C. miR195 suppresses metastasis and angiogenesis of squamous cell lung cancer by inhibiting the expression of VEGF. *Mol Med Rep* 2019; 20: 2625-2632.
- 18) CAO W, ZHAO Y, WANG L, HUANG X. Circ0001429 regulates progression of bladder cancer through binding miR-205-5p and promoting VEGFA expression. *Cancer Biomark* 2019; 25: 101-113.
- 19) TAN Z, CHEN K, WU W, ZHOU Y, ZHU J, WU G, CAO L, ZHANG X, GUAN H, YANG Y, ZHANG W, LI J. Overexpression of HOXC10 promotes angiogenesis in human glioma via interaction with PRMT5 and upregulation of VEGFA expression. *Theranostics* 2018; 8: 5143-5158.